

Folded and Unfolded Conformations of the ω -3 Polyunsaturated Fatty Acid Family: $\text{CH}_3\text{CH}_2[\text{CH}=\text{CHCH}_2]_B[\text{CH}_2]_M\text{COOH}$. First Principles Study

Jacqueline M. S. Law,^{†,‡} Milan Szori,[‡] Robert Izsak,[‡] Botond Penke,[§] Imre G. Csizmadia,^{†,‡} and Bela Viskolcz^{*‡}

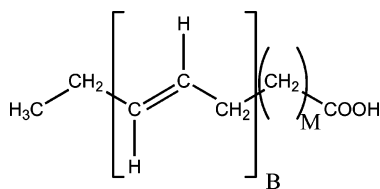
Department of Chemistry, University of Toronto, ON, Canada M5S 3H6, Department of Chemistry and Chemical Informatics, Faculty of Education, University of Szeged, Szeged, Boldogasszony sgt. 6, Hungary 6725, and Protein Chemistry Research Group, Hungarian Academy of Sciences, University of Szeged, Dóm tér 8, Szeged, Hungary 6720

Received: August 3, 2005

Polyunsaturated fatty acids (PUFA) like stearidonic acid (SDA; 18:4 n-3) eicosapentaenoic acid (EPA; 20:5 n-3), and docosahexaenoic acid (DHA; 22:6 n-3) and its chain fragment models were studied at B3LYP/6-31G(d) levels of theory. Significant conformations for the *cis* and *trans* isomers were selected to obtain the thermodynamic functions (ΔH , ΔS , ΔG) for the *cis*–*trans* isomerization and for folding using the B3LYP/6-311+G(2d,p)/B3LYP/6-31G(d) level of theory. The structural analysis shows that there are significant differences in thermodynamic function of the *trans*- and *cis*-PUFAs. The *trans*–*cis* isomerization energy values reinforce the consistency and the relative accuracy of theoretical model calculations. The observed flexibility of naturally *cis* PUFAs could be explained by a very special “smooth basin” PES of the motif of sp^2 – sp^3 – sp^2 hybrid states as reported previously (*J. Phys. Chem. A* 2005, 109, 520–533). We assumed that intrinsic thermodynamic functions may describe this flexible folding process. The folding enthalpy as well as the folding entropy suggests that there is a new role of the *cis*-PUFAs in membranes: these *cis* isomers may have a strong influence on membrane stability and permeability. The average length of the *cis* helix and beta PUFA was approximated. The difference between the lengths of these two structures is approximately 10 Å.

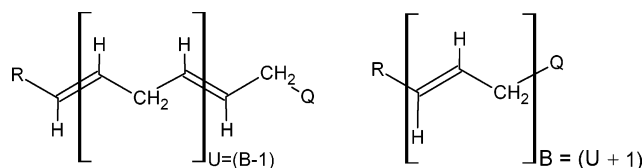
Introduction

Polyunsaturated fatty acids (PUFAs) play significant roles in many biological processes. Their significance is underlined by the introduction of the new term lipomics.^{1,2} This terminology is based on the notion that lipids plus genomics equals lipomics. An important subclass of PUFAs, called n-3 or ω -3 fatty acids, are characterized by their double bond network which starts from the third carbon atom counting from the methyl carbon at the tail end (ω end) of the fatty acid.



The structures of different ω -3 PUFA species vary in the number (B) of allylic blocks (denoted as B) in the chain and in the number of CH_2 units (M) connecting the polyallylic chain to the carboxyl group. For example, docosahexaenoic acid (DHA; 22:6 n-3) contains six B blocks and one M unit (i.e., $B = 6$ and $M = 1$). The most frequently occurring ω -3 fatty acids are listed in Table 1. Evaluating the structural composition shown in Table 1, it is clear that the number of B blocks is equal to the number of double bonds. However, there are one fewer

($U = B - 1$) highly activated CH_2 units (denoted as B) sandwiched between two olefinic double bonds.



Although there are many ways in which the PUFA chains may be modeled, in this study, the polyallylic chain is retained and only the end groups are varied. In a previous study³ all models contain the groups $R = \text{CH}_3$ and $Q = \text{H}$. However, they vary in the number of n and N values, and thus, they were labeled as U (e.g., $3U$, $4U$, $5U$) or B (e.g., $4B$, $5B$, $6B$) and referred to as model 0. In the present study, two sets of model compounds were selected. The first set (model 1) has the following end groups: $R = \text{CH}_3\text{CH}_2$ and $Q = \text{CH}_3$. Therefore R in model 1 is the same length as all the ω -3 fatty acids, and the length of Q is fixed with the methyl group. Thus, all members in this model contain CH_3CH_2 as their terminal groups, and they are labeled nU' (e.g., $3U'$, $4U'$, $5U'$) or NB (e.g., $4B'$, $5B'$, $6B'$). In the second set (model 2), R is identical with that of model 1 (i.e., $R = \text{CH}_2\text{CH}_3$) for all members in this set, but Q in different structures ($(\text{CH}_2)_M\text{H}$) will vary to mimic the chain length of the three PUFAs studied. Therefore, M may be 1, 2, and 3. This set of structures with varying unsaturated chain length were labeled as nU'' (e.g., $3U''$, $4U''$, $5U''$) or NB'' (e.g., $4B''$, $5B''$, $6B''$). Table 2 lists relevant compounds investigated in the previous and present studies. Three ω -3 fatty acids, denoted as stearidonic acid (SDA; 18:4 n-3), eicosapentaenoic

* Corresponding author: viskolcz@jgytf.u-szeged.hu.

[†] University of Toronto.

[‡] University of Szeged.

[§] University of Szeged.

TABLE 1: Structural Information and Biosynthetic Pathway^a of Frequently Occurring ω -3 (or n-3) Fatty Acids^b

Scientific Names of PUFA	Structural Composition Symbols C:B; ω	Common Names of Acids	2D Structures
9,12,15-octadecatrienoic	C ₁₈ H ₃₀ O ₂ 18:3; ω -3	α -linolenic (ALA)	
6,9,12,15-octadecatetraenoic	C ₁₈ H ₂₈ O ₂ 18:4; ω -3	stearidonic (SDA)	
11,14,17-eicosatrienoic	C ₂₀ H ₃₄ O ₂ 20:3; ω -3	eicosatrienoic (EtrA)	
8,11,14,17-eicosatetraenoic	C ₂₀ H ₃₂ O ₂ 20:4; ω -3	eicosatetraenoic (ETA)	
5,8,11,14,17-eicosapentaenoic	C ₂₀ H ₃₀ O ₂ 20:5; ω -3	eicosapentaenoic (EPA)	
7,10,13,16,19-docosapentaenoic	C ₂₂ H ₃₄ O ₂ 22:5; ω -3	docosapentaenoic (DPA)	
4,7,10,13,16,19-docosahexaenoic	C ₂₂ H ₃₂ O ₂ 22:6; ω -3	docosahexaenoic (DHA)	
9,12,15,18,21-tetracosapentaenoic acid	C ₂₄ H ₃₈ O ₂ 24:5; ω -3	Tetracosapentaenoic (TPA)	
6,9,12,15,18,21-tetracosahexaenoic	C ₂₄ H ₃₆ O ₂ 24:6; ω -3	Tetracosahexaenoic (THA)	
$ \begin{array}{ccccccc} & \Delta 6 & & \text{Elongase} & & \Delta 5 & & \text{Elongase} & & \text{Elongase} & & \Delta 6 & & \beta\text{-oxidation} \\ 18:3 \ \omega\text{-3} & \longrightarrow & 18:4 \ \omega\text{-3} & \longrightarrow & 20:4 \ \omega\text{-3} & \longrightarrow & 20:5 \ \omega\text{-3} & \longrightarrow & 22:5 \ \omega\text{-3} & \longrightarrow & 24:5 \ \omega\text{-3} & \longrightarrow & 24:6 \ \omega\text{-3} & \longrightarrow & 22:6 \ \omega\text{-3} \\ \text{ALA} & & \text{SDA} & & \text{ETA} & & \text{EPA} & & \text{DPA} & & \text{TPA} & & \text{THA} & & \text{DHA} \\ \downarrow \text{Elongase} & & & & & & & & & & & & & & \\ 20:3 \ \omega\text{-3} & & & & & & & & & & & & & & \\ \text{EtrA} & & & & & & & & & & & & & & \end{array} $			

^a Symbols $\Delta 6$ and $\Delta 5$ indicate the introduction of a CC double bond at the positions 6 and 7 and positions 5 and 6, respectively. Elongase is the enzyme which executes the elongation of the carbon chain. ^b The numbering of the carbon atoms is in accordance with the IUPAC convention, which is different from the computational numbering presented in Figure 1.

TABLE 2: Structural Comparison of Selected ω -3 Fatty Acids with Their Hydrocarbon Models

chain length			CH ₃ [CH=CHCH ₂] _N H ^b model 0 nU or NB	CH ₃ CH ₂ [CH=CHCH ₂] _N CH ₂ H model 1 nU' or NB'	CH ₃ CH ₂ [CH=CHCH ₂] _N (CH ₂) _M H model 2 nU'' or NB''	CH ₃ CH ₂ [CH=CHCH ₂] _N (CH ₂) _M COOH PUFA ^a	
B	U = (B - 1)	M					
4	3	3	<i>cis</i> -3U or 4B <i>trans</i> -3U or 4B	<i>cis</i> -3U' or 4B' <i>trans</i> -3U' or 4B'	<i>cis</i> -3U'' or 4B'' <i>trans</i> -3U'' or 4B''	<i>cis</i> -SDA <i>trans</i> -SDA	C ₁₈ H ₂₈ O ₂
5	4	2	<i>cis</i> -4U or 5B <i>trans</i> -4U or 5B	<i>cis</i> -4U' or 5B' <i>trans</i> -4U' or 5B'	<i>cis</i> -4U'' or 5B'' <i>trans</i> -4U'' or 5B''	<i>cis</i> -EPA <i>trans</i> -EPA	C ₂₀ H ₃₀ O ₂
6	5	1	<i>cis</i> -5U or 6B <i>trans</i> -5U or 6B	<i>cis</i> -5U' or 6B' <i>trans</i> -5U' or 6B'	<i>cis</i> -5U'' or 6B'' <i>trans</i> -5U'' or 6B''	<i>cis</i> -DHA <i>trans</i> -DHA	C ₂₂ H ₃₂ O ₂

^a SDA = stearidonic acid [CAS Registry No. 20290-75-9]. EPA = eicosapentaenoic acid [CAS Registry No. 10417-94-4]. DHA = docosahexaenoic acid [CAS Registry No. 6217-54-5]. ^b Reference 3.

acid (EPA; 20:5 n-3), and docosahexaenoic acid (DHA; 22:6 n3), shown in Table 2, were also studied. Model 1, model 2, and PUFA structures are shown in Figure 1A, Figure 1B, and Figure 1C, respectively.

Structural Features. Although extensive research has been carried out to study the metabolism of EPA and DHA and their roles in health and disease, it was not until recently that rigorous investigations were performed on the physical and conformational properties of these important ω -3 PUFAs. Common methods employed for physical and structural analysis of DHA, EPA, and other PUFAs include ¹³C NMR and ¹H NMR spectroscopy, molecular dynamics (MD), and molecular mechanics (MM). In spectroscopy, ¹³C NMR is often used to identify specific PUFA species in samples^{4,5} through the detection of the degrees of unsaturation.^{6,7} In fact, this method is so sensitive that it is able to determine even the positions (α or C₁ and β or C₂ position) of fatty acids in the glycerol ester. In one study, using ¹³C NMR, it was revealed that the distribution of EPA in α and β positions in triacylglycerol is

about the same, but DHA is found predominantly on the β position.⁸

The latter methods, including ²H NMR, MD, and MM, are often used for structural studies. ²H NMR is popular in determining the general order and movement of EPA in a bilayer system. For example, Paddy's study of lipid bilayer order using ²H NMR spectroscopy has suggested that bilayers with phospholipids containing either DHA or palmitoleic acid are much more deformable than bilayers with only saturated acids.⁹ On the other hand, MD and MM are utilized for PUFA structural and conformational analysis. Therefore, using MM, Applegate and Glomset predicted not only the possible conformations of DHA and analogues but also the patterns of chains packing within a phospholipid and/or with a lipid bilayer.^{10,11}

A simple strategy was developed to study such complicated systems, and the present paper is divided into two essential parts: (i) conformational characterization of the chains of PUFA models as well as SDA, EPA, and DHA; (ii) computations of

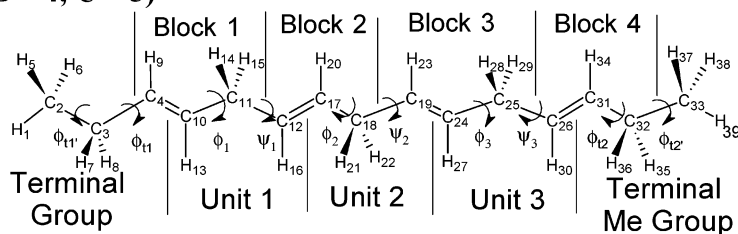
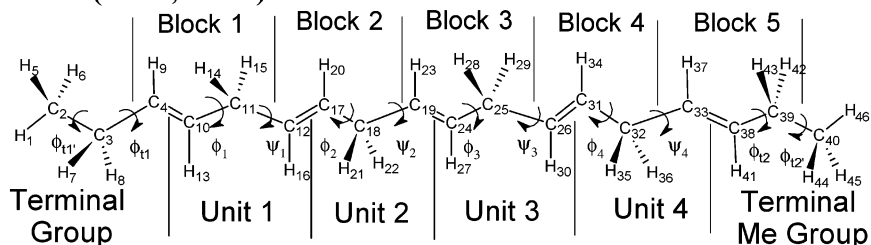
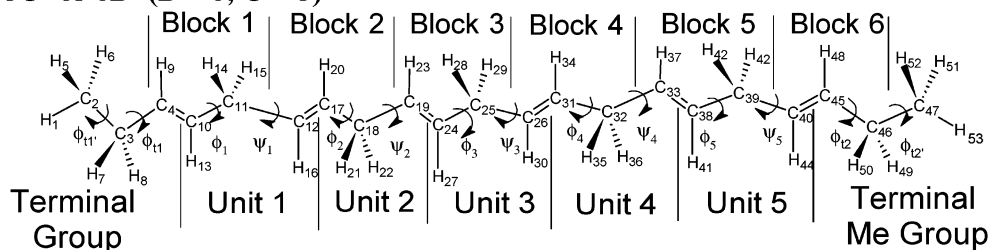
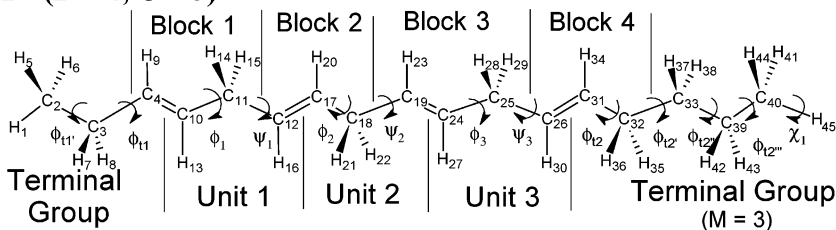
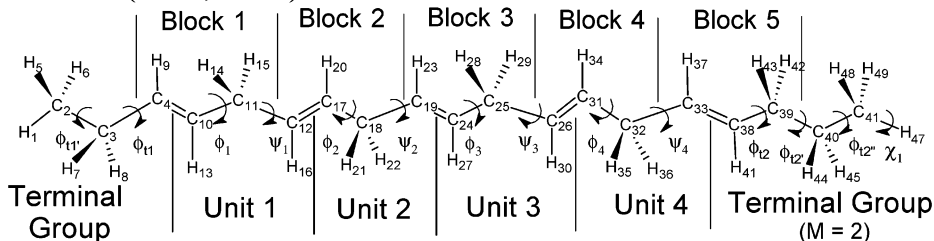
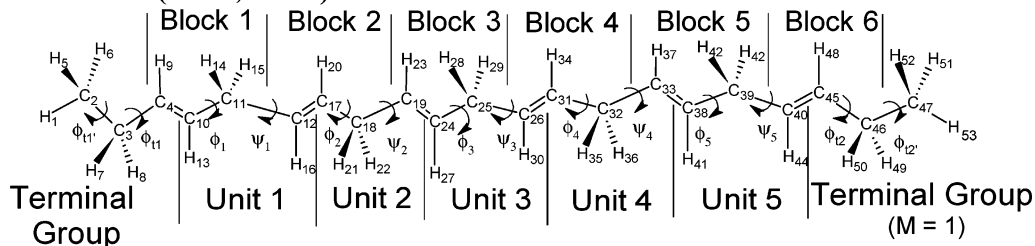
3U' or 4B' (B = 4; U = 3)**4U' or 5B' (B = 5; U = 4)****5U' or 6B' (B = 6; U = 5)****3U'' or 4B'' (B = 4; U = 3)****4U'' or 5B'' (B = 5; U = 4)****5U'' or 6B'' (B = 6; U = 5)**

Figure 1. (Continued)

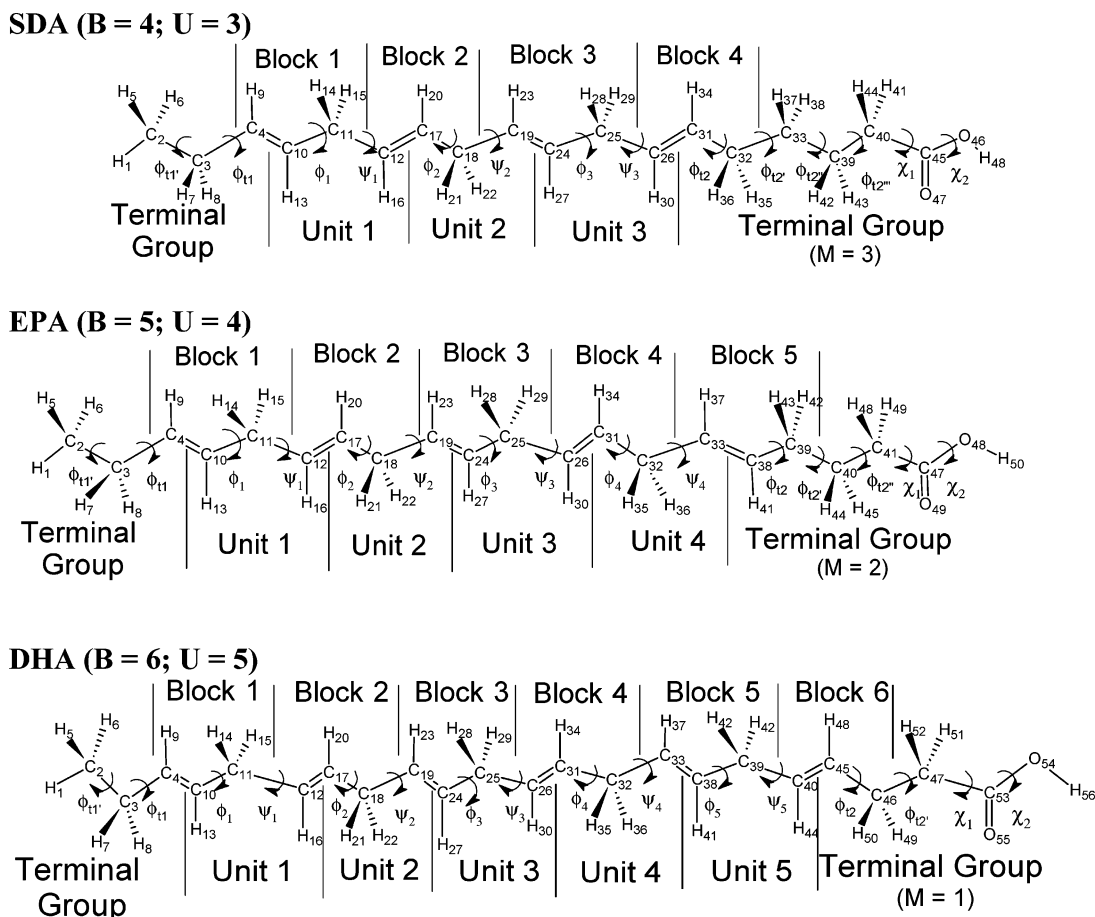


Figure 1. (A) Structures of model 1 with fixed chain length ($R = \text{Et}$, $Q = \text{Me}$, and $M = 0$); only the *trans* isomers are shown. **B** gives the number of blocks, and **U** specifies the number of units. The numbering in this figure does not correspond to the IUPAC convention. (B) Structures of model 2 with variable chain length ($R = \text{Et}$ and $Q = (\text{CH}_2)_M\text{H}$ with $M = 3, 2, \text{ and } 1$); only the *trans* isomers are shown. **B** gives the number of blocks, and **U** specifies the number of units. The numbering in this figure does not correspond to the IUPAC convention. (C) Structures of selected PUFAs (SDA, EPA, and DHA with $R = \text{Et}$ and $Q = (\text{CH}_2)_M\text{COOH}$ with $M = 3, 2, \text{ and } 1$); only the *trans* isomers are shown. **B** gives the number of blocks, and **U** specifies the number of units. The numbering of PUFAs is made not to meet IUPAC convention but to have a one to one correspondence to previous models shown in Figures 1A and 1B.

the thermodynamic functions (ΔU , ΔH , ΔG , and S) of PUFA models as well as SDA, EPA, and DHA.

Methods

Model Compounds. Models 1 and 2 as well as selected ω -3 PUFAs, shown in Figure 1A, Figure 1B, and Figure 1C, respectively, were numbered modularly according to the numbering system previously developed.¹² Models 1 and 2 were selected to see if the conformational intricacy of the hydrocarbon chain could be studied and understood without the carboxyl functionality. All correspondent *cis* and *trans* isomers of models and PUFAs have the same number of double bonds at the same positions. For the present study, three conformations were selected. They include two straight chains and one helical conformation as shown in Figure 2. The beta conformers of both the *cis* and *trans* families were the most stable, and they were used as a reference structure. The optimized dihedral angles for the hydrocarbon backbone and the end groups are listed in Supplementary Table 1a and Supplementary Table 1b, respectively (Supporting Information).

Molecular Computation. Geometry optimizations and frequency calculations were performed at B3LYP/6-31G(d) levels of theory. The ZPEs were scaled using the factor of 0.96.¹³ The thermodynamic functions (ΔH , ΔS , ΔG) were obtained at the

B3LYP/6-311G(2d,p)//B3LYP/6-31G(d) level of theory. Calculations were conducted using the Gaussian03 program packages.¹⁴

Isomerization and Folding Energies. The *trans*–*cis* isomerizations for all three models were calculated with respect to the lowest conformation, which, in this case, was usually the conformation with $\phi_i = \psi_i \sim 120^\circ$; $\phi_{i+1} = \psi_{i+1} \sim -120^\circ$. Then, for all models, the *trans*–*cis* isomerization and folding energies were calculated using eqs 1 and 2, respectively. The other

$$\Delta E_{\text{isom}} = E_{\text{cis}} - E_{\text{trans}} \quad (1)$$

$$\Delta E_{\text{folding}} = E_{\text{helix}} - E_{\text{beta}} \quad (2)$$

thermodynamic functions (ΔH , ΔS , and ΔG) were computed for the *trans*–*cis* isomerization and for the folding (Figure 3) in an analogous fashion. Figure 3 is a Born–Haber thermodynamic cycle which relates thermodynamic function defined in accordance with eqs 1 and 2. The relative enthalpy values are shown in Figure 4.

Results and Discussion

Despite such rapid structural research and development, still only very little is known about how the structures of these PUFAs are related to their precise functions in the membrane

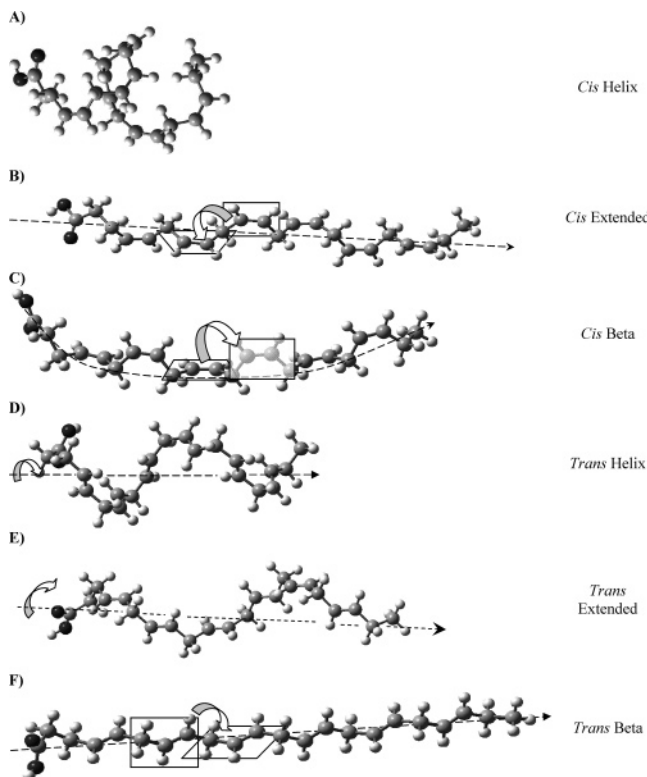


Figure 2. (a) Side view of the DHA chain optimized by the B3LYP/6-31G(d) level of theory and (b) top view of the DHA chain. Structures A to F are the *cis* helix, *cis* extended, *cis* beta, *trans* helix, *trans* extended, and *trans* beta structures, respectively.

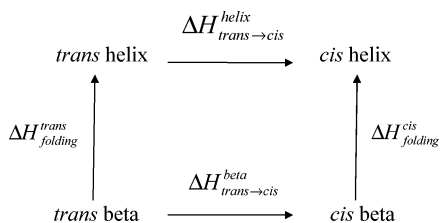
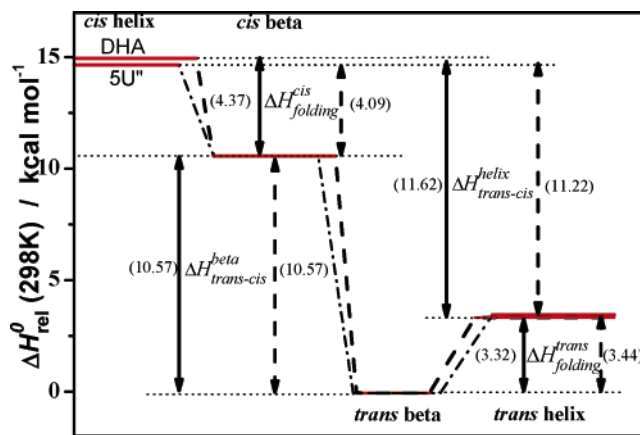


Figure 3. Born-Haber enthalpy cycle for configurational and conformational changes of PUFA as well as their hydrocarbon models

and micelles. As a result, this makes conformational/structural analysis and prediction an indispensable part of lipid research.¹⁵



PUFA Conformers

Figure 4. Enthalpy diagram for the Born-Haber thermodynamic cycle associated with the configurational and conformational change of DHA as well as its $n = 5$ hydrocarbon model.

Larger structural units such as helices of proteins or glycogen carry essential information to understand structural biology. It has been shown that the number of possible conformers increases significantly with the number of internal rotors. However, results in *in vivo* systems show that only a few of the conformers play an important role. As one attempts to understand the elusive protein folding mechanism, one must question how these few conformers are selected and evaluated from the large ensemble of conformers that may exist for a large molecule. The situation is analogous in lipid structural research. On closer inspection, DHA shows that its structural formula is very similar to a glyceryl oligopeptide, namely, both contain $[sp^2-sp^2-sp^3]$ bonding.³ Consequently, it was interesting to compare *trans*- and *cis*-DHA models to peptide folding models.³ The chain of the DHA model contains no heteroatoms, and its chain structure has no intramolecular hydrogen bonds, unlike polypeptide chains. One of the aims of the present paper is to show some thermodynamic properties of folding of selected PUFA models and actual ω -3 PUFAs including DHA.

In many ω -3 PUFAs, like DHA, all double bonds exist in *cis* configuration. However, *trans*-DHA can be synthesized by heating of *cis*-linolenic acid into *trans*-linolenic followed by elongation to *trans*-DHA.¹⁶ With such a high degree of unsaturation, DHA is very susceptible to oxidation by free radicals.¹⁷ Rabinovitch and Ripatti argued¹⁸ that a polyunsaturated chain having double-bonded carbons separated by a single methyl group, the motif found in DHA, has “maximum flexibility” and is minimally sensitive to temperature. This increased flexibility allows it to fold easily into various secondary structures.¹⁹ However, when incorporated into a lipid bilayer, the flexibility of DHA may reduce the strength of the lipid bilayer and increase its water permeability.²⁰ On the other hand, molecular mechanics (MM) computer modeling studies of DHA have been interpreted as suggesting a more rigid and ordered character for the polyunsaturated DHA chain.²¹ Previous conformational studies had been carried out on small fragments resembling *cis*-DHA and other DHA analogues using MM methods.²¹ They suggested that the planes of the double bonds are nearly perpendicular to each other.^{18,21–25} With the present *ab initio* and DFT study we will show that the DHA structure has greater flexibility than the earlier MM calculations have suggested.²¹

Secondary structural motifs such as extended, β -sheet, and helix conformations were studied for both the *trans* and *cis*

TABLE 3: ZPE Corrected Relative Energy and Enthalpy, Gibbs Free Energy (kcal mol⁻¹), and Entropy (cal (mol K)⁻¹) for ω -3 PUFAs and Their Model Compounds Obtained by B3LYP Density Function Combined with 6-31G(d) (A) and 6-311+G(2d,p) Basis Sets

model	structure	ΔE_0 B3LYP/A	ΔE_0 B3LYP/B	ΔH_0 B3LYP/B	ΔG_0 B3LYP/B	S_0 B3LYP/A	ΔS_0 B3LYP/A	
Model 1 Fixed Chain Length for Q (Me) with $M = 0$								
<i>cis</i> -3U'	helix	9.0	9.6	9.4	9.4	147.2	-3.1	
	extended	7.1	7.1	7.0	6.0	150.3	-0.1	
	beta	7.1	7.2	7.0	6.1	150.4	0.0	
<i>trans</i> -3U'	helix	1.7	2.0	2.1	1.6	148.6	1.4	
	extended	-0.1	-0.1	-0.1	-0.7	149.1	1.9	
	beta	0.0	0.0	0.0	0.0	147.2	0.0	
-585.983283, -585.631166 ^a	<i>cis</i> -4U'	helix	11.3	12.2	11.9	12.7	165.7	-5.8
	extended	8.8	8.9	8.7	7.7	171.4	-0.1	
	beta	8.9	9.0	8.8	7.8	171.5	0.0	
<i>trans</i> -4U'	helix	2.3	2.8	2.8	2.9	167.9	-0.4	
	extended	0.0	-0.1	-0.1	-0.8	170.8	2.5	
	beta	0.0	0.0	0.0	0.0	168.3	0.0	
-702.693033, -702.279039 ^a	<i>cis</i> -5U' ^b	helix	13.6	15.1	14.7	15.9	184.9	-7.8
	extended	10.7	10.7	10.5	9.1	193.7	0.9	
	beta	10.8	10.9	10.6	9.5	192.8	0.0	
<i>trans</i> -5U' ^b	helix	2.9	3.5	3.4	3.4	189.5	0.3	
	extended	0.0	0.0	-0.1	-0.6	191.1	1.8	
	beta	0.0	0.0	0.0	0.0	189.2	0.0	
Model 2 Variable Chain Length for Q with $M = 3, 2, \text{ and } 1$								
<i>cis</i> -3U''	helix	8.7	9.1	8.9	7.9	155.5	-3.3	
	extended	7.1	7.2	6.9	6.3	157.9	-0.9	
	beta	7.1	7.1	7.0	5.5	158.8	0.0	
<i>trans</i> -3U''	helix	1.8	2.2	2.1	2.6	156.1	1.2	
	extended	0.0	0.0	-0.1	-0.4	157.0	2.1	
	beta	0.0	0.0	0.0	0.0	154.9	0.0	
-664.610897, -664.201574 ^a	<i>cis</i> -4U''	helix	11.1	12.1	11.8	12.9	174.2	-5.6
	extended	8.9	9.0	8.7	8.6	178.5	-1.3	
	beta	9.0	9.1	8.8	8.4	179.8	0.0	
<i>trans</i> -4U''	helix	2.4	2.9	2.8	3.1	177.3	-0.8	
	extended	0.0	0.0	0.0	-0.2	178.6	0.5	
	beta	0.0	0.0	0.0	0.0	178.1	0.0	
-742.006937, -741.564445 ^a	<i>cis</i> -5U'' ^b	helix	13.6	15.1	14.7	15.9	184.9	-7.8
	extended	10.7	10.7	10.5	9.1	193.7	0.9	
	beta	10.8	10.9	10.6	9.5	192.8	0.0	
<i>trans</i> -5U'' ^b	helix	2.9	3.5	3.4	3.4	189.5	0.3	
	extended	0.0	0.0	-0.1	-0.6	191.1	1.8	
	beta	0.0	0.0	0.0	0.0	189.2	0.0	
ω -3 Polyunsaturated Fatty Acids (PUFAs)								
<i>cis</i> -SDA	helix	8.2	9.8	9.4	11.5	175.5	-5.8	
	extended	7.1	7.2	6.9	6.6	183.3	2.0	
	beta	7.3	7.3	7.0	7.3	181.3	0.0	
<i>trans</i> -SDA	helix	1.7	2.1	2.0	2.6	180.5	-1.8	
	extended	0.1	0.1	0.0	0.2	181.4	-0.8	
	beta	0.0	0.0	0.0	0.0	182.3	0.0	
-853.176842, -852.752487 ^a	<i>cis</i> -EPA	helix	10.2	12.1	11.7	13.9	186.3	-10.5
	extended	9.0	9.1	8.8	8.3	195.3	-1.5	
	beta	9.0	9.1	8.8	7.9	196.8	0.0	
<i>trans</i> -EPA	helix	2.2	2.7	2.6	2.7	193.4	-0.3	
	extended	-0.1	0.1	-0.1	-0.4	194.8	1.2	
	beta	0.0	0.0	0.0	0.0	193.7	0.0	
^a -930.572706, -930.114895 ^a	<i>cis</i> -DHA	helix	12.9	15.5	14.9	17.2	198.0	-11.8
	extended	10.6	10.7	10.5	8.4	212.7	2.9	
	beta	10.7	10.9	10.6	9.3	209.8	0.0	
<i>trans</i> -DHA	helix	2.8	3.4	3.3	3.0	206.9	1.2	
	extended	0.0	-0.1	-0.1	-1.3	209.7	4.0	
	beta	0.0	0.0	0.0	0.0	205.7	0.0	

^a Energy (in hartree) of the *trans* beta conformation in all structures. Left: energy. Right: energy with zero point correction. ^b 5U' and 5U'' models are identical.

isomers of all model compounds as well as for the three PUFA structures: SDA, EPA, and DHA. The three model families involved differ from each other in their terminal groups, and the three families are denoted³ as *nU* and *nU'* as well as *nU''*. Thus, all three families and the PUFA structures can be compared.

Conformations of Model 1 and Model 2 and the ω -3 PUFA Family. A total of nine structures from model 1, model

2, and PUFA were first optimized at RHF/3-21G and subsequently at B3LYP/6-31G(d) levels of theory in various conformations. Relative energy values are recorded in Table 3 and illustrated in Figure 4 for DHA and 5U''. Figure 5 contains all of the dihedral values found in each unit. This topological diagram is analogous to a "Ramachandran map" used in peptide chemistry. Assessment of these values shows that most of them are tightly clustered. This implies that all points within a cluster

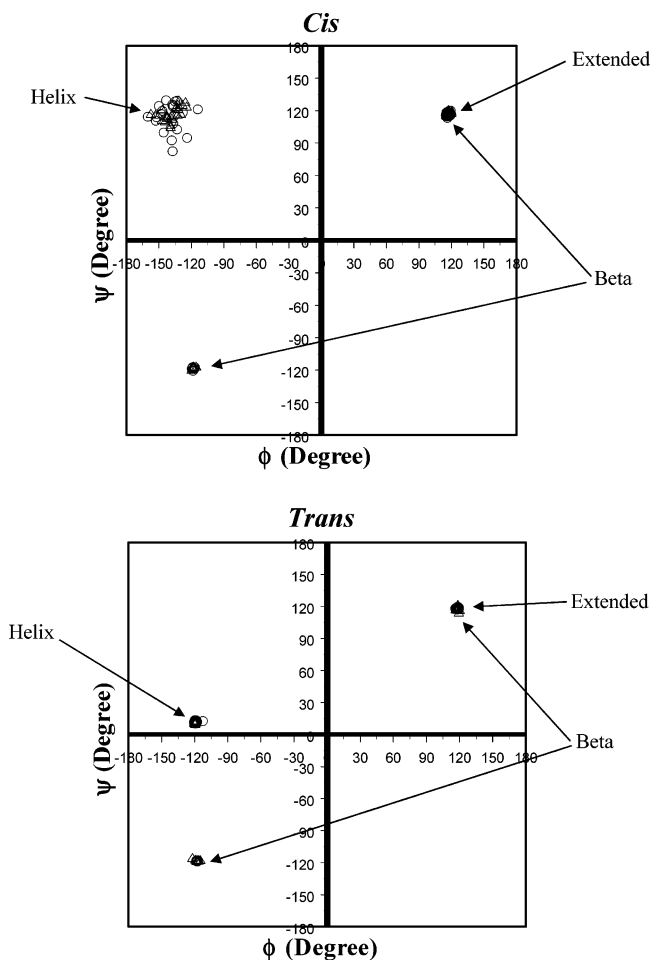


Figure 5. Topological map of all points in ϕ/ψ coordinates from all $n\mathbf{U}$ (represented by triangles), $n\mathbf{U}'$, and $n\mathbf{U}''$ models and PUFA (SDA, EPA, and DHA are represented by circles). All *cis* and all *trans* conformers are included in the upper and the lower part of the figure, respectively.

TABLE 4: Definition of the Structures Being Studied in Models 0, 1, and 2 and PUFA

definition	indices ^a ($\phi_i, \psi_i, \phi_{i+1}, \psi_{i+1}$)
<i>trans</i> beta	+, +, -, -
<i>trans</i> extended	+, +, +, +
<i>trans</i> helix ^b	-, s ⁺ , -, s ⁺
<i>cis</i> beta	+, +, -, -
<i>cis</i> extended	+, +, +, +
<i>cis</i> helix ^b	-, +, -, +

^a The following symbols are used to indicate approximate conformations: +, g⁺ (gauche⁺ between +60° and +180°); -, g⁻ (gauche⁻ between -60° and -180°); s⁺, syn⁺ (small positive value, close to zero). ^b In the *trans* helix the ψ values shifted to values close to zero while in the *cis* helix ψ values are between +60° and +180° as illustrated in Figure 5.

are conformationally equivalent. The chosen structures (extended + + + +, beta + + - -, and helix - + - + shown in Table 4) are constructed by repeatedly using the values from the appropriate clusters.

These six structures (three *cis* and three *trans*), shown in Figure 2, exhibit striking similarities to those previously found,³ consisting of only a single methyl ending in the terminal groups. Therefore, they are also named *cis* helix (A), *cis* extended (B), *cis* beta (C), *trans* helix (D), *trans* extended (E), and *trans* beta (F). Like the model from the previous paper, these chains with

methyl terminal groups also require four units to make one helical turn.

Comparison between $4\mathbf{U}'$, $5\mathbf{U}'$, and DHA shows that, with the exception of the *cis* helix structures, all other structures for all models have very similar dihedral ϕ values as defined in Figure 1. In the *cis* helix however, only the ϕ values are very similar for the first two units. In the third unit, the ϕ_3 of $4\mathbf{U}'$ deviates from the other two models. This implies that the similarity of $5\mathbf{U}'$ is more to DHA than that of $4\mathbf{U}'$ (with deviation of $\pm 3^\circ$ in the ϕ dihedrals). A closer inspection shows that the ϕ dihedral values can be divided into different ranges. In unit 1 and unit 2, the range is between 130° and 135° , and in units 3 and 4, the range is between 140° and 145° . The value of the fifth unit is back in the first range. Conversely, there is no visible correlation of ψ values within a given *cis* helix structure.

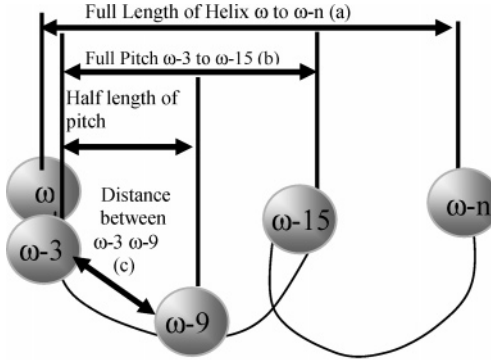
The dihedral values of the terminal groups are all similar for the same structures across all models. Comparison of terminal group dihedral values between different structures in a given model shows that $\phi_{1'}$ and $\phi_{2'}$ are in the staggered position while the ϕ_{11} and ϕ_{12} are in the eclipsed position for most structures. However, ϕ_{11} for the *cis* helix of all models is skewed from the eclipsed position to $130^\circ \pm 1^\circ$. In addition, the carboxyl group of the *cis* helix χ_1 and the terminal group of ϕ_{12} is also skewed from the expected value of $180^\circ \pm 2^\circ$.

Nanostructural Characteristic Structure of Model 1, Model 2, and the ω -3 PUFA Family. To calculate the nanostructural properties from the molecular parameters for the various secondary structures, the same reference atoms were selected. The distance of corresponding atoms in different structures can be defined as a diameter, and the length (or half-length) of the turn as is shown in Table 5. Characteristics of the helical structure and other secondary structure are defined and summarized in Table 5. Since ω dihedrals in these structures can only be in syn or anti conformation, they are similar to the planes of the amide linkage that formed along the polypeptide chain. Also, since in straight chains there are no turns and coils, the degree of twist on its own axis becomes very important in determining the available space around the molecule as well as the shape of the PUFA. In turn, such a macromolecular property may also affect the packing order of the lipid bilayers. The twists are described as the rotation of the allylic planes, and they are measured by obtaining the dihedral as shown in the top figure of Table 6. The variation of the average twists and their standard deviations are also shown in Table 6. To calculate these values, the absolute value is taken for each measurement. Then, the average and the standard deviation of all these absolute values in one structure are taken. The results show that, for all straight chains, the plane rotation is about 90° . In the *cis* helix, the rotational dihedral is 30° on average, and the *trans* helix is around 105° . In both structures, the standard deviations for the rotation of the plane are very small for all structures except for the *cis* helix. Once again, this observation is in good agreement with the variation of the *cis* helix conformation seen earlier.

The names of the unsaturated hydrocarbon components are reminiscent of peptide secondary structures such as α -helix and β -sheet. The *trans* beta conformation is a geometrical entity which is fairly similar to a single stranded beta conformation of a peptide chain. However, the *cis* isomer is considerably twisted as illustrated by the rotation of the planes associated with adjacent double bonds. This is illustrated in Figure 6.

Geometric Isomers. The fully *trans* isomers always are more stable than the corresponding *cis* isomers for all secondary

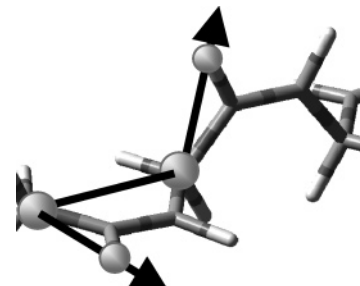
TABLE 5: Nanostructural Parameters (Length, Pitch, and Diameter in Å) for ω -3 PUFAs and Their Model Compounds^a



model	structure	length of chain (a)	pitch (b)	distance between C _{ω-3} and C _{ω-9} (c)	diameter (d)
Model 1 Fixed Chain Length for Q (Me) with M = 0					
<i>cis</i> -3U'	helix	5.9	5.3	5.9	5.3
	extended	14.9			
<i>trans</i> -3U'	beta	14.7			
	helix	11.4	9.2	6.4	4.4
<i>cis</i> -4U'	extended	14.3			
	beta	16.0			
<i>trans</i> -4U'	helix	7.3	5.3	5.8	5.2
	extended	18.1			
<i>cis</i> -5U'	beta	17.9			
	helix	12.9	10.2	6.8	4.5
<i>trans</i> -5U'	extended	14.4			
	beta	19.5			
<i>cis</i> -3U''	helix	9.5	6.0	5.9	5.1
	extended	21.3			
<i>trans</i> -3U''	beta	21.3			
	helix	15.6	9.2	6.3	4.3
<i>cis</i> -4U''	extended	20.3			
	beta	22.2			
Model 2 Variable Chain Length for Q with M = 3, 2, and 1					
<i>cis</i> -3U''	helix	7.8	5.3	5.9	5.3
	extended	17.1			
<i>trans</i> -3U''	beta	16.7			
	helix	13.6	9.3	6.3	4.3
<i>cis</i> -4U''	extended	16.4			
	beta	18.5			
<i>trans</i> -4U''	helix	8.0	5.6	5.7	5.0
	extended	19.1			
<i>cis</i> -5U''	beta	18.7			
	helix	14.1	9.0	6.3	4.4
<i>trans</i> -5U''	extended	18.4			
	beta	20.4			
ω -3 Polyunsaturated Fatty Acids (PUFAs)					
<i>cis</i> -SDA	helix	7.3	5.1	6.1	5.5
	extended	18.2			
<i>trans</i> -SDA	beta	17.9			
	helix	14.5	9.1	6.3	4.4
<i>cis</i> -EPA	extended	17.5			
	beta	19.6			
<i>trans</i> -EPA	helix	9.3	5.5	6.1	5.4
	extended	20.2			
<i>cis</i> -DHA	beta	20.1			
	helix	14.4	9.0	6.4	4.5
<i>trans</i> -DHA	extended	19.4			
	beta	22.0			
<i>cis</i> -DHA	helix	9.2	5.2	5.9	5.3
	extended	22.2			
<i>trans</i> -DHA	beta	22.4			
	helix	17.0	9.2	6.4	4.4
<i>cis</i> -DHA	extended	21.5			
	beta	23.5			

^a 5U' and 5U'' models are identical.

TABLE 6: Average Plane Rotation Values and Standard Deviation (deg)



model	structure	av angle of plane rotation (deg)	std dev
Model 1 Fixed Chain Length for Q (Me) with M = 0			
<i>cis</i> -3U'	helix	34.5	8.2
	extended	-93.0	0.1
<i>trans</i> -3U'	beta	92.9	0.5
	helix	-105.5	0.6
<i>cis</i> -4U'	extended	93.4	0.2
	beta	93.2	0.2
<i>trans</i> -4U'	helix	35.6	16.4
	extended	-93.5	0.2
<i>cis</i> -5U'	beta	92.7	0.4
	helix	-105.4	0.9
<i>trans</i> -5U'	extended	93.2	0.2
	beta	93.1	0.1
<i>cis</i> -3U''	helix	29.5	16.4
	extended	-93.2	0.7
<i>trans</i> -3U''	beta	93.0	0.8
	helix	-105.5	1.2
<i>cis</i> -4U''	extended	92.5	0.5
	beta	93.0	0.2
Model 2 Variable Chain Length for Q with M = 3, 2, and 1			
<i>cis</i> -3U''	helix	28.6	18.8
	extended	-94.3	0.5
<i>trans</i> -3U''	beta	93.1	1.6
	helix	-105.4	1.3
<i>cis</i> -4U''	extended	94.1	0.3
	beta	93.0	0.5
<i>trans</i> -4U''	helix	42.2	19.8
	extended	-93.0	1.1
<i>cis</i> -5U''	beta	92.4	0.5
	helix	-105.3	0.7
<i>trans</i> -5U''	extended	92.6	0.2
	beta	92.7	1.3
ω -3 Polyunsaturated Fatty Acids (PUFAs)			
<i>cis</i> -SDA	helix	25.2	20.5
	extended	-93.1	0.1
<i>trans</i> -SDA	beta	92.3	0.8
	helix	-104.9	1.0
<i>cis</i> -EPA	extended	93.4	0.3
	beta	93.2	0.5
<i>trans</i> -EPA	helix	15.5	10.2
	extended	-94.2	0.3
<i>cis</i> -DHA	beta	92.1	1.3
	helix	-104.7	0.8
<i>trans</i> -DHA	extended	92.5	0.6
	beta	93.0	0.4
<i>cis</i> -DHA	helix	35.2	16.9
	extended	-94.1	0.4
<i>trans</i> -DHA	beta	92.8	0.5
	helix	-105.3	0.6
<i>cis</i> -DHA	extended	93.4	0.3
	beta	34.5	8.2

structural motifs. The thermodynamic functions for *trans* to *cis* isomerization are the following:

$$\Delta H_{trans \rightarrow cis} = H_{cis} - H_{trans}$$

$$\Delta S_{trans \rightarrow cis} = S_{cis} - S_{trans}$$

$$\Delta G_{trans \rightarrow cis} = \Delta H_{trans \rightarrow cis} - T\Delta S_{trans \rightarrow cis}$$

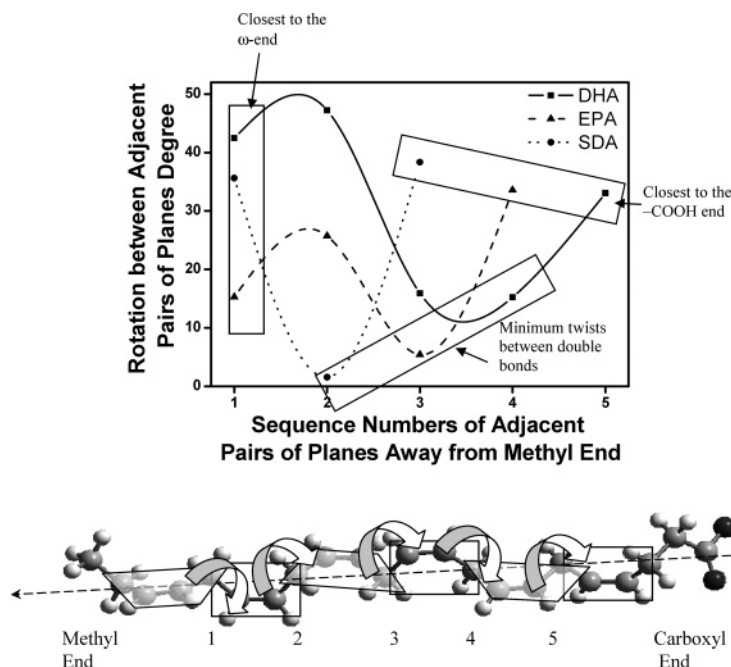


Figure 6. Rotation of adjacent planes of *cis* double bonds as a function of position in the chain of the *cis* helix form. The three curves represent different periodicities for the various PUFAs of different degrees of polymerization ($n = 4$ for SDA, $n = 5$ for EPA, and $n = 6$ for DHA).

TABLE 7: Energy of *Trans* → *Cis* Isomerization and Energy of Folding for Model 1, Model 2, and PUFA

compound	structure	<i>trans</i> → <i>cis</i> isomerization			folding beta → helix	
		helix	extended	beta	<i>cis</i>	<i>trans</i>
model 1	3U'	7.3	7.1	7.0	2.4	2.1
	4U'	9.2	8.7	8.8	3.2	2.8
	5U'	11.2	10.5	10.6	4.1	3.4
model 2	3U''	6.8	7.0	7.0	1.9	2.1
	4U''	8.9	8.7	8.8	2.9	2.8
	5U''	11.2	10.5	10.6	4.1	3.4
PUFA	SDA	7.4	7.0	7.0	2.4	2.0
	EPA	9.1	8.8	8.8	2.9	2.6
	DHA	11.6	10.5	10.6	4.4	3.3

The values of these thermodynamic functions are expected to change, virtually monotonically with increasing degree of polymerization (N) as may be measured by nU (the number of diallylic CH_2 units) or by $(n + 1)B$ (the number of allylic blocks in the polymer since $N = n + 1$). This is clearly seen in Table 7.

Figure 7 shows the variation of $\Delta H_{\text{trans} \rightarrow \text{cis}}$, $\Delta S_{\text{trans} \rightarrow \text{cis}}$, and $\Delta G_{\text{trans} \rightarrow \text{cis}}$ as a function of the number of units (n) in the polyunsaturated chain. Interestingly enough, both the *trans* and *cis* isomers of the three model families (nU , nU' , and nU'') as well as the *trans* isomer of the PUFA family (SDA, EPA, and DHA) yield a fairly accurate straight line for the $\Delta H_{\text{trans} \rightarrow \text{cis}}$ values (see top panel of Figure 7). However, the *cis* isomers of the PUFA family (SDA, EPA and DHA) have lower value than predicted by the fitted straight line. This means that some stabilization is present in these helices having *cis* double bonds, since the formation of these helical secondary structures are less endothermic. Obviously, the presence of the COOH terminal group could exert some stabilizing interaction which is present only in the *cis* helical structure.

Since the effect of the terminal COOH group on the conformation of the PUFA chain is relatively minor, it is assumed that the conformational study of the hydrocarbon chain will also be relevant to PUFA derivatives. For example, the carboxyl group (COOH) may be deprotonated to COO^- , to a certain degree, depending on its pK_a value, at physiological pH.

Also, the COOH group may be esterified to COOR in triglycerides or in phospholipids. In these derivations only slight structural modifications are anticipated to occur. In both of these cases similar conformational patterns are expected to dominate as in the case of the parent carboxylic acid.

The bottom panel of Figure 7 shows the variation of ΔS with n . The central panel of Figure 7 illustrates the combined effects of ΔH and ΔS as manifested in ΔG , also as a function of the degree of polymerization as measured by n . Table 8 summarizes the slope, y -intercepts, and R^2 of the *trans*–*cis* isomerization of model 1, model 2, and PUFA.

Conformational Folding. The extent of folding is measured by the change of thermodynamic functions ($\Delta H_{\text{folding}}$, $\Delta S_{\text{folding}}$, and $\Delta G_{\text{folding}}$) on going from the most extended to the most densely packed helix conformation. Such motion represents a considerable conformational change between extreme secondary structural motifs.

$$\Delta H_{\text{folding}} = H_{\text{helix}} - H_{\text{extended}}$$

$$\Delta S_{\text{folding}} = S_{\text{helix}} - S_{\text{extended}}$$

$$\Delta G_{\text{folding}} = \Delta H_{\text{folding}} - T\Delta S_{\text{folding}}$$

Table 7 and Figure 8 shows the variation of these thermodynamic functions with increasing number of units (n) in the polyunsaturated chain. The pattern of $\Delta H_{\text{folding}}$ (top panel of Figure 8) is analogous to that of $\Delta H_{\text{trans} \rightarrow \text{cis}}$ isomerization.

However, the stabilization for EPA as measured by its $\Delta H_{\text{folding}}$ value, with respect to those of the models (nU , nU' , nU''), is slightly different. For the *trans* → *cis* isomerization it is about 1.77 kcal/mol, and for the extended → helix folding it is about 1.00 kcal/mol.

The combined enthalpy changes may be summarized in a Born–Haber thermodynamic cycle shown in Figure 3. The corresponding enthalpy level diagram is shown in Figure 4 for $n = 5$ as well as for DHA illustrating the stabilization achieved by the helical *cis*-PUFAs.

The bottom panel of Figure 8 shows the variation of $\Delta S_{\text{folding}}$. For the *trans* isomers there is a minimal change in entropy.

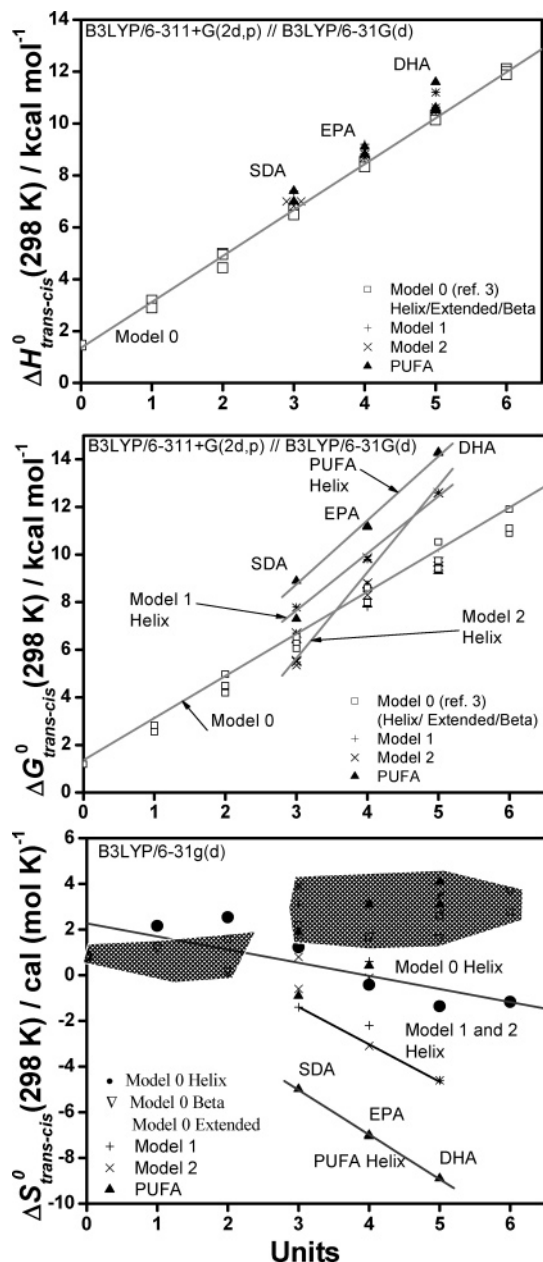


Figure 7. Thermodynamic functions (ΔH , ΔG , and ΔS) of the *cis* and *trans* isomerization as a function of the number of units. Points in the shaded area show no apparent correlation.

Nevertheless, there is a trend for the *trans* isomers since its $\Delta S_{\text{folding}}$ exhibits a slight change toward negative values indicating that the helical form is slightly more ordered than the extended form. In contrast to the above, the change in $\Delta S_{\text{folding}}$ for the *cis* isomers is considerably more pronounced even for the hydrocarbon models. Clearly the $\Delta S_{\text{folding}}$ assumes the lowest negative values for the longest PUFA (i.e., DHA). Again EPA derivatives from the SDA–DHA line indicate further internal interaction for EPA.

Recalling that in our previous paper some analogy was found concerning the flexibility of these *cis* polyunsaturated chains and *trans*-peptides, we may anticipate an analogous entropy lowering for helical secondary structures of oligopeptides. The central panel of Figure 8 shows the variation of $\Delta G_{\text{folding}}$. Table 8 contains a summary of $\Delta H_{\text{folding}}$, $\Delta G_{\text{folding}}$, and $\Delta S_{\text{folding}}$ graphs.

Table 3 contains in addition to the relative energy values all thermodynamic functions for the three ω -3 PUFA structures as

TABLE 8: Linear Trends for All Helices' *Trans*–*Cis* Isomerization and *Cis* Folding of All Models^a

thermodynamic function	model	<i>m</i>	<i>b</i>	<i>R</i> ²
<i>Trans</i> → <i>Cis</i> Isomerization for Helices				
ΔH	0 ^b	1.8	1.4	1.00
	1	1.8	1.4	1.00
	2	1.8	1.4	1.00
	PUFA	1.8	1.4	1.00
ΔG	0 ^b	1.7	1.1	0.99
	1	5.2	3.6	0.98
	2	2.4	0.5	0.99
	PUFA	2.7	0.7	0.99
ΔS	0 ^b	−1.9	4.4	0.99
	1	−1.6	3.6	0.95
	2	−1.6	3.6	0.95
	PUFA	−2.0	0.8	1.00
<i>Cis</i> ^c Folding				
ΔH	0 ^b	0.7	−0.1	0.98
	1	0.9	0.2	1.00
	2	1.1	−1.4	0.99
ΔG	PUFA	1.0	−0.8	0.92
	0 ^b	0.8	−0.2	0.94
	1	1.5	1.1	1.00
ΔS	2	2.0	−3.5	0.99
	PUFA	1.9	−1.4	1.00
	0	−1.9	4.4	0.99
	1	−2.3	3.8	0.99
	2	−2.3	3.8	0.99
	PUFA	−3.0	2.7	0.91

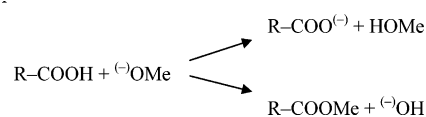
^a The linear fit equation is as follows: $y = mx + b$. ^b Helix, extended, and beta isomers follow the same trend. ^c *Cis* and *trans* isomers follow the same trend.

well as their hydrocarbon models in all their conformations studied. Not surprisingly, the data shows that every *trans* conformer is more stable than its *cis* pair. In accordance with Benson's group additivity rules,²⁶ the relationship between the relative energy of *trans*–*cis* isomers of the allylic molecules and the degree of polymerization was also investigated. As was suggested earlier,²⁷ the additivity rule is an excellent and sensitive tool to estimate the change in accuracy with the molecular size.

Various PUFAs such as DHA have three major types of functional groups: the carboxylic acid functionality, the carbon–carbon double bonds, and the allylic C–H bonds. Of these three functionalities the COOH group is the most easily changeable. It can deprotonate easily leading to an anionic function group: COO^(−). However, it can also be esterified as it occurs in triglycerides and phospholipids. The simplest ester that might be considered is the methyl ester. In order to make a preliminary assessment of how the state of the carboxyl group may influence the folding of the carbon skeleton and associated energetics, we compared the three states of the *cis* isomer of DHA using all three conformations studied (extended, helix, and beta).



The thermodynamic functions for the three conformers of the three states of the carboxyl functionality are summarized in Table 9, and Figure 9 shows the enthalpy changes of these nine structures in two pseudoisodesmic reactions:



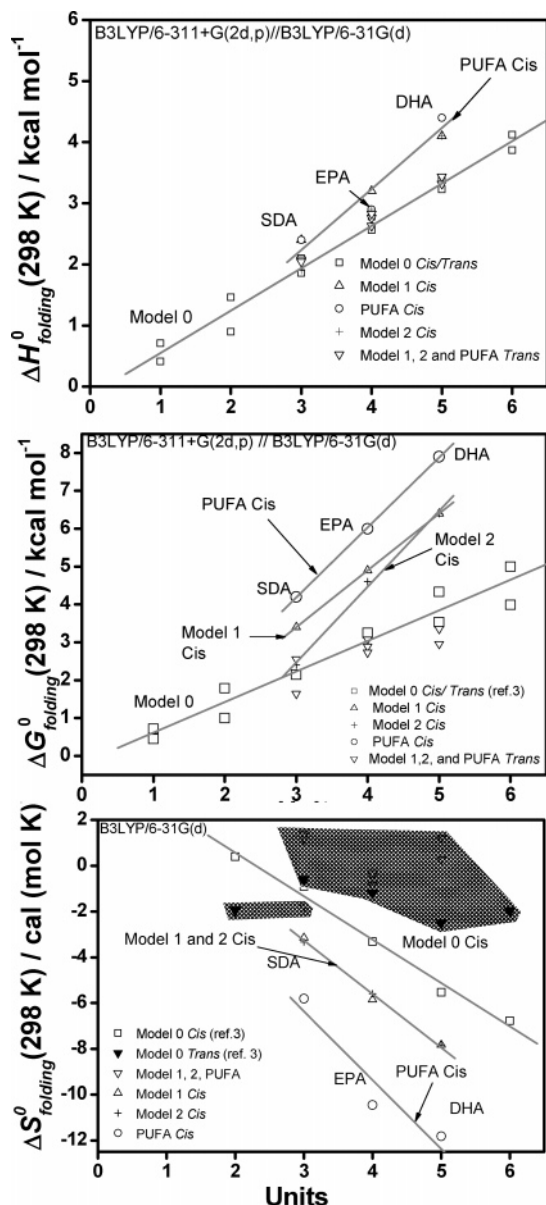


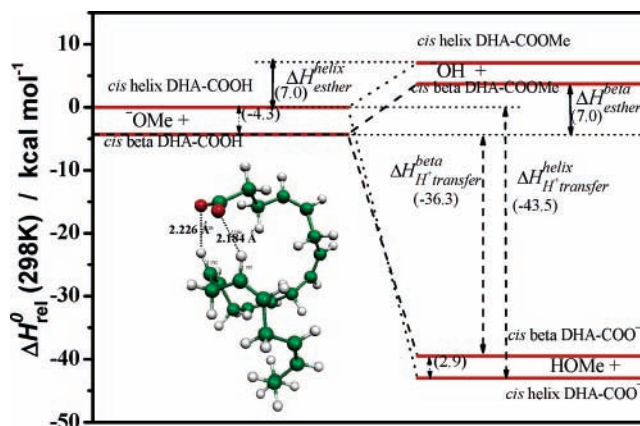
Figure 8. Thermodynamic functions (ΔH , ΔG , and ΔS) of folding vs number of units. Points in the shaded area show no apparent correlation.

TABLE 9: The Relative Energy, Enthalpy, Gibbs Free Energy (kcal mol^{-1}), and Entropy (cal (mol K)^{-1}) for the Proton Transfer and Esterification Reactions of *cis*-DHA^a

model	structure	ΔE_0 B3LYP/B	ΔH_0 B3LYP/B	ΔG_0 B3LYP/B	ΔS_0 B3LYP/A
$\text{R-COOH} + (^-)\text{OMe} \rightarrow \text{R-COO}^{(-)} + \text{HOME}$					
<i>cis</i> -DHA-COO ⁻	helix	-43.5	-43.5	-43.1	-1.3
	extended	-38.7	-38.7	-38.4	-2.2
	beta	-38.6	-38.7	-38.3	1.7
$\text{R-COOH} + (^-)\text{OMe} \rightarrow \text{R-COOMe} + (^-)\text{OH}$					
<i>cis</i> -DHA-COOCH ₃	helix	6.4	7.1	8.5	-4.7
	extended	7.0	7.0	8.4	-6.2
	beta	7.0	7.0	8.4	-3.2

^a Values for ΔS_0 were obtained by B3LYP density functional theory combined with the 6-31G(d) [A] basis set, and values for ΔE_0 , ΔH_0 , and ΔG_0 were calculated using the 6-311+G(2d,p) [B] basis set.

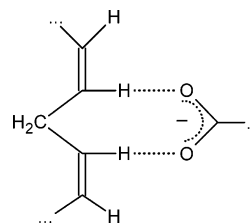
Note that the “beta” conformer is indistinguishable from the “extended” isomer on the scale of Figure 9. The enthalpy change on going from the acid state to the ester state is relatively small, and the associated geometry change is practically negligible. In contrast to that, the enthalpy change, on going from the acid



Ionization and Esterification Process of DHA

Figure 9. Enthalpies of proton transfer and esterification of the neutral *cis*-DHA conformers. Note that the beta and extended DHA conformers are indistinguishable on the scale of the figure.

state to the anion state, is rather large (in the vicinity of 40 kcal/mol). Furthermore, the less stable the *cis*-acid became, the more stable the *cis*-anion was. This extra stabilization was associated with the large geometry change and the formation of some hydrogen bonds involving vinylic C–H bonds:



Clearly, such an intramolecular hydrogen bonded structure is typical of the gaseous phase. The two $\text{CH}\cdots\text{O}$ hydrogen bond lengths (2.184 and 2.226 Å) shown in Figure 9 represent non-negligible interactions. In fact, they are similar in strength to $\text{NH}\cdots\text{O}$ interactions that hold peptides in helical conformations.^{28,29} Such a comparison between PUFAs and peptides has already been made.³

Conclusion

For this study and the previous study, the conformations of the select structures are very similar. This implies that the structures chosen for all models in both studies are the same ones and, therefore, are comparable. Furthermore, this is also evidence that suggests that in a single molecule the terminal groups have little to no effect on the conformation of the unit. Also, the ϕ conformational trend observed in DHA and **5U'** *cis* helices shows that the first half of the turn is structurally different from the second half. Therefore, this helix is asymmetrical. However, no observable trends can be found in the ψ dihedral angles.

In energy analysis, comparison between *cis* helices of **4U'**, **5U'**, and DHA shows that there is additional stabilization occurring in the DHA structure. This stabilization force is also observed in *trans*–*cis* isomerization energy and folding energy. Although it is not clear which interaction is involved, comparison of relative energy values between DHA and **5U'** shows that this additional stabilization is only observable in the DHA *cis* helices. In earlier analysis, it has already been suggested that interaction between nonadjacent groups is most likely to occur in *cis* helices. The fact that this unique stabilization force occurs

only in DHA *cis* helices may mean that it is a form of nonadjacent interaction. A closer inspection of terminal and carboxyl group dihedrals shows that ϕ_{12} and χ_1 of the DHA *cis* helix have values lower than other structures in DHA. This may be a clue which can lead to pinpointing the specific interactions which result in the additional stabilization force.

Acknowledgment. This research was supported by the National Science Fund of Hungary (OTKA T046861 and F037648). One of us (I.G.C.) wishes to thank the Ministry of Education for a Szent-Györgyi Visiting Professorship. We wish to thank for computational time at University of Szeged (MU-00094/2002). The authors would also like to thank M. Labadi for technical support and also Suzanne Lau for helpful discussion.

Supporting Information Available: Supplementary Tables 1a and 1b listing optimized dihedral angles for the hydrocarbon backbone and the end groups. This material is available free of charge via the Internet at <http://pubs.acs.org>.

References and Notes

- (1) German J. B.; Roberts M. A.; Watkins S. M. *J. Nutr.* **2003**, *133*, 4260–4266.
- (2) Fitzgerald D. A. *Scientist* **2002**, *16*, 42–42.
- (3) Law J. M. S.; Setiadi, D. H.; Chass, A. G.; Csizmadia, I. G.; Viskolcz B. *J. Phys. Chem. A* **2005**, *109*, 520–533.
- (4) Fu, M.; Koulman, A.; van Rijssel, M.; Lutzen, A.; de Boer, M. K.; Tyl, M. R.; Liebezit, G. *Toxicol* **2004**, *43*, 355–363.
- (5) Sacchi, R.; Medina, I.; Paolillo, L.; Addeo, F. *Chem. Phys. Lipids* **1994**, *69*, 65–73.
- (6) Aursand, M.; Grasdalen, H. *Chem. Phys. Lipids* **1992**, *62*, 239–251.
- (7) Gunstone, F. D.; Seth, S.; Wolff, R. L. *Chem. Phys. Lipids* **1995**, *78*, 89–96.
- (8) Gunstone, F. D.; Seth, S. *Chem. Phys. Lipids* **1994**, *72*, 119–126.
- (9) Paddy, M. R.; Dahlquist, F. W. *Biochemistry* **1985**, *24*, 5988–5995.
- (10) Applegate, K. R.; Glomset, J. A. *J. Lipid Res.* **1991**, *32*, 1635–1644.
- (11) Applegate, K. R.; Glomset, J. A. *J. Lipid Res.* **1991**, *32*, 1645–1655.
- (12) Law J.; Chass, G. A.; Torday, L. L.; Varro, A. Papp, J. Gy. *THEOCHEM* **2002**, *619*, 1–20.
- (13) Scott, A. P.; Radom, L., *J. Phys. Chem.* **1996**, *100*, 16502–16513.
- (14) Frisch, M. J.; Trucks, G. W.; Schlegel, H. B.; Scuseria, G. E.; Robb, M. A.; Cheeseman, J. R.; Montgomery, J. A., Jr.; Vreven, T.; Kudin, K. N.; Burant, J. C.; Millam, J. M.; Iyengar, S. S.; Tomasi, J.; Barone, V.; Mennucci, B.; Cossi, M.; Scalmani, G.; Rega, N.; Petersson, G. A.; Nakatsuji, H.; Hada, M.; Ehara, M.; Toyota, K.; Fukuda, R.; Hasegawa, J.; Ishida, M.; Nakajima, T.; Honda, Y.; Kitao, O.; Nakai, H.; Klene, M.; Li, X.; Knox, J. E.; Hratchian, H. P.; Cross, J. B.; Bakken, V.; Adamo, C.; Jaramillo, J.; Gomperts, R.; Stratmann, R. E.; Yazyev, O.; Austin, A. J.; Cammi, R.; Pomelli, C.; Ochterski, J. W.; Ayala, P. Y.; Morokuma, K.; Voth, G. A.; Salvador, P.; Dannenberg, J. J.; Zakrzewski, V. G.; Dapprich, S.; Daniels, A. D.; Strain, M. C.; Farkas, O.; Malick, D. K.; Rabuck, A. D.; Raghavachari, K.; Foresman, J. B.; Ortiz, J. V.; Cui, Q.; Baboul, A. G.; Clifford, S.; Cioslowski, J.; Stefanov, B. B.; Liu, G.; Liashenko, A.; Piskorz, P.; Komaromi, I.; Martin, R. L.; Fox, D. J.; Keith, T.; Al-Laham, M. A.; Peng, C. Y.; Nanayakkara, A.; Challacombe, M.; Gill, P. M. W.; Johnson, B.; Chen, W.; Wong, M. W.; Gonzalez, C.; Pople, J. A. *Gaussian 03*, revision A.1; Gaussian, Inc.: Pittsburgh, PA, 2003.
- (15) Mitchell, D. C.; Gawrisch, K.; Litman, B. J.; Salem, N., Jr. *Mol. Struct. Phospholipids Regul. Cell Funct.* **1998**, *26*, 365–370.
- (16) Acar, N.; Chardigny, J.; Bonhomme, B.; Almanza, S.; Doly, M.; Sébédio, J. *J. Nutr.* **2002**, *132*, 3151–3154.
- (17) Alexander-North, L. S. North, J. A.; Kiminyo, K. P.; Buettner, G. R.; Spector, A. A., *J. Lipid Res.* **1994**, *35*, 1773–1785.
- (18) Rabinovich, A. L.; Ripatti, P. O. *Biophys. Biochim. Acta* **1991**, *1085*, 53–62.
- (19) Feller, S. E.; Gawrisch, K.; MacKerell, A. D. *J. Am. Chem. Soc.* **2002**, *124*, 318–326.
- (20) Olbrich, K.; Rawicz, W.; Needham, D.; Evans, E.; *Biophys. J.* **2000**, *79*, 321–327.
- (21) Applegate, K. R.; Glomset, J. A. *J. Lipid Res.* **1986**, *27*, 658–680.
- (22) Shimanouchi, T.; Abe, Y.; Alaki Y. *Bull. Chem. Soc. Jpn.* **1971**, *48*, 3557–3560.
- (23) Schurinck, W. T.; de Jong, S. *Chem. Phys. Lipids* **1977**, *19*, 313–322.
- (24) Albrand, M.; Pageaux, J.; Lagarde, M.; Dolmazon, R. *Chem. Phys. Lipids* **1994**, *72*, 7–17.
- (25) van Hemelrijk, D.; van den Enden L.; Geise, H. J. *J. Mol. Struct.* **1981**, *74*, 123–135.
- (26) Benson, S. W. *Thermochemical Kinetics*; John Wiley and Sons: New York, 1976.
- (27) Marsi, I.; Viskolcz, B.; Seres, L. *J. Phys. Chem. A* **2000**, *104*, 4497–4504.
- (28) Topol, I. A.; Burt, S. K.; Deretey, E.; Tang, T.-H.; Perczel, A.; Rashin, A.; Csizmadia, I. G. *J. Am. Chem. Soc.* **2001**, *123*, 6054–6060.
- (29) Tang, T.-H.; Deretey, E.; Knak Jensen, S. J.; Csizmadia, I. G. *Eur. Phys. J. D* **2005** [e2005-00317-0].